ELSEVIER

Journal of Nuclear Materials 299 (2001) 157–164

journal of nuclear materials

www.elsevier.com/locate/jnucmat

Microstructure–fracture toughness relationship of vanadium alloy/stainless steel brazed joints

Y.X. Gan [a], H.A. Aglan [a,*], R.V. Steward [b,1], B.A. Chin [b], M.L. Grossbeck [c]

[a] *Mechanical Engineering Department, Tuskegee University, Tuskegee, AL 36088, USA*
[b] *Materials Engineering Program, 201 Ross Hall, Auburn University, Auburn, AL 36849, USA*
[c] *Oak Ridge National Laboratory, Oak Ridge, TN 37831, USA*

Received 19 January 2001; accepted 2 August 2001

Abstract

In this work, brazing V–5Ti–5Cr to 304 stainless steel (SS 304) using Au–18Ni alloy as filler material was conducted under high vacuum condition. Sessile drop technique was used to determine the wettability of filler alloy to the stainless steel and the vanadium alloy substrates upon which the relationship between the contact angles with time was obtained. Tensile tests were performed on unnotched and notched specimens to demonstrate the overloading behavior and the fracture toughness of the base materials and the brazed joint. Fracture surface was examined for both the V–5Ti–5Cr and the joint to identify the failure mechanisms under static loadings. It was found that the Au–18Ni filler material exhibited good wettability with the SS 304 and V–5Ti–5Cr. The ultimate tensile strength of the brazed joint reached 245 MPa. The strain to failure was about 1.3%. Young's modulus was about 351 GPa. The fracture toughness (K_{Ic}) of this joint was 19.1 MPa $\sqrt{}$m. The fracture surface of the joint showed well brazed area with good wettability and proper amount of residual filler material which came from the solidification of residual liquid filler alloy of Au–Ni. The failure of the joint occurred along the interface of the vanadium/filler under static load. © 2001 Published by Elsevier Science B.V.

1. Introduction

Currently, brazing technology has been successfully used in joining first wall components [1–9]. Rodij et al. [1] have reported to join flat tile mock-ups using Ti as filler material. Plasma facing tubular walls have been brazed to the heat sinking layer using Pd, Ni, Zr, Pd–Ni, Pd–Co as fillers [2–7]. Although refractory materials such as W, Mo, SiC, B_4C_3, C/C, and Si_3N_4 are extensively studied as plasma facing armor materials [10–22], vanadium alloys are considered as promising candidate materials for the first wall and blanket components of fusion reactors [23]. Vanadium alloys have several advantages over other metallic alloys and/or ceramics including good thermal conductivity at high temperatures, good mechanical properties at both ambient and elevated temperatures, low activation characteristics, chemical compatibility with liquid metals such as lithium, sodium, Li–Pb alloy, Bi–Pb alloy, and Bi–In–Sn ternary alloy [24–26]. Among various vanadium alloy systems, V–(3–6)Ti–(3–6)Cr has been considered. This alloy system possesses very good formability which is essential for the large scale engineering applications [27].

Joining vanadium alloys to lower cost dissimilar metallic alloys or non-metallic materials is critical for the construction of cost-effective power generating systems. Grossbeck and King [28,30] and Grossbeck et al. [29] have investigated the gas-tungsten arc (GTA) welding of vanadium alloys and preliminary results have been reported. One of the shortcomings related to GTA welding process is the embrittlement of the heat affected zone (HAZ). It has been demonstrated by Potluri et al. [31] that significant hardening occurred in the HAZ of a vanadium alloy produced under simulated GTA using

* Corresponding author. Tel.: +1-334 727 8973; fax: +1-334 727 8090.
E-mail address: aglanh@acd.tusk.edu (H.A. Aglan).
[1] Currently with Georgia Institute of Technology.

0022-3115/01/$ - see front matter © 2001 Published by Elsevier Science B.V.
PII: S0022-3115(01)00677-8

controlled Gleeble weld thermal history cycles. Laser welding of vanadium alloys has also been studied [32–35]. In order to reduce interstitial contaminants in vanadium weldments, solid state methods by which no inert gas is used have been developed. These include the resistance welding, explosive bonding and initial bonding as proposed by Johnson and Trester [36], and the diffusion bonding as proposed by Xu et al. [37]. Brazing has some advantages in joining dissimilar materials. These include good wettability, small heat affected zone, low residual stress, minimized distortion and reduced chemical incompatibility of the dissimilar materials [38,39]. The feasibility of brazing vanadium alloys to stainless steel (SS) was demonstrated by Liu et al. [39] using BCu-1 as filler alloy. BCu-7 was also used as filler and the brazement was found more brittle than the former. More recently, different fillers have been identified for brazing vanadium to SS 304 [38,40,41].

There are several brazing techniques developed for commercial applications among which induction brazing, torch brazing and furnace brazing are very common [42–47]. Induction brazing employs an electro-magnetic field to generate heat necessary for joining. The advantage of induction brazing is selective heating which allows a lot of equipment to be joined by this method [47]. In torch brazing process, fuel gas flame is furnished to generate the required heat to melt the filler alloys. Torch brazing has several advantages. It is suitable for joining odd configured parts such as tubes and shells. The equipment used is handy and manually portable. Besides, dissimilar materials can be brazed by properly choosing joining locations and controlling the procedure and amount of heat. That is the reason that torch brazing has been widely used in various industrial fields including air conditioning, refrigerator, heat exchanger, compressor, and plumbing [42,44]. Unlike the two brazing processes mentioned above, furnace brazing is operated in capsulated environment. In this process, components and filler materials are pre-located and placed in a furnace. Vacuum or inert gas protection are normally used in the brazing. In some cases, purging the furnace with an inert gas to provide a low partial pressure atmosphere may also be adopted to alleviate possible high temperature corrosion. In furnace brazing, heating and cooling parameters in the whole process can be precisely controlled which allows the brazing operation with high reproducibility and in consistence [42,44].

There are several criteria for selection of brazing fillers and evaluation on the quality of brazed joints. The fluidity of filler to permit its distribution by capillary action into properly prepared joints is one of these criteria which determines the wettability of filler materials to the matrix materials [48]. Static tensile test on the brazed material system is one of the direct ways of evaluation on the joining quality [49]. Fracture toughness (K_{Ic}) is also one of the parameters which can be used to characterize the brazed joints. It relies on the residual strength of the material with defects, the geometrical factor of the structure and the stress singularity. In this work, brazing V–5Ti–5Cr to 304 stainless steel (SS 304) using a high vacuum furnace was conducted. The wettability of Au–18Ni filler to both vanadium alloy and stainless steel was determined by sessile drop technique. Static tests were performed on unnotched and notched specimens from the base alloys and the brazed joint. Microscopic examination of the fracture surface of the brazement was performed as well.

2. Materials and experimental methods

Various brazing alloys or fillers for joining dissimilar materials have been investigated [50–57]. However, fillers designed for joining vanadium alloys have not been fully identified. In this work, a commercially available Au–Ni alloy filler was used. Butt joint was formed at brazing temperature of 970 °C. The vacuum used is 10^{-4} to 10^{-5} Pa. Details in the brazing experiment was described in [38,40,41]. Sessile drop experiment was conducted to determine the contact angle, θ, which is used for the evaluation of the wettability. The composition of the filler and brazing conditions are summarized in Table 1. The chemical composition for the above filler is based on weight percentage. From Table 1, it can be seen that the brazing temperature for this system is approximately 20 °C above the melting point of the filler alloy.

The butt joint of V–5Ti–5Cr/Au–Ni/SS 304 was cut by electric discharging machining (EDM) along the longitudinal direction into specimens with 1 mm thickness for tensile tests. Unnotched specimens were tested for generating stress–strain curve of the joint. Notched specimens were tested for obtaining the residual strength and fracture toughness of the joint. For notched specimens, a 60° V-shaped notch with a radius less than 0.05 mm was machined at the center of one free edge of the specimens. The notch depth is about 3.0 mm and the notch depth to sample width ratio (a/w) is 0.46. The

Table 1
Composition of the filler and the brazing conditions

Filler	Composition	Melting point	Brazing temperature	Holding time	Ramp rate	Cooling rate
Au–Ni	Au18Ni	950 °C	970 °C	5 min	10 °C/min	10 °C/min

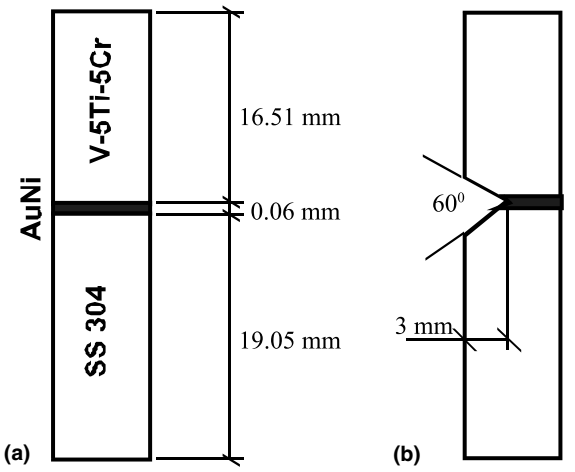

Fig. 1. The geometries of tensile specimens from the V–5Ti–5Cr/Au–Ni/SS 304 brazed joint: (a) unnotched specimen; (b) notched specimen.

geometries of both notched and unnotched specimens are shown in Figs. 1(a) and (b), respectively.

V–5Ti–5Cr and SS 304 specimens were also prepared and tested. The V–5Ti–5Cr was purchased from Wah Chang, Albany, OR, with the heat number of 832394. The supplied alloy was in the form of warm rolled plate [27]. The stainless steel was cut from a cold rolled plate. In order to identify the difference in strength and toughness of the base materials and the brazed joints, the base alloys were put in the some thermal history before the mechanical tests. Thus, both the stainless steel and the vanadium alloy were heated up to the brazing temperature of 970 °C in a ramp rate of 10 °C/min, held at 970 °C for 5 min and cooled down to room temperature in a cooling rate of 10 °C/min. This state for the two base materials is called 'as-processed'.

Static tensile tests were performed at room temperature of 25 °C using a materials testing system (MTS 810) equipped with a 100 kN load cell. The specimens were griped between two hydraulic wedge grips. All the specimens of the base alloy and the brazed V–5Ti–5Cr/304 stainless steel joint were tested under displacement control with a crosshead speed of 1.5 mm/min. The fracture surface of the V–5Ti–5Cr and the joint after failure under static loadings was examined using a Hitachi S-2150 scanning electron microscope operated at an acceleration voltage of 25 kV.

3. Results and discussion

3.1. Wettability of filler

Experiments were conducted on both the Au–18Ni filler/SS 304 side and the filler/V–5Ti–5Cr side to study the wettability of the filler. Results concerning the melting and wetting action of Au–18Ni on stainless steel and on V-5Cr-5Ti were generated. The contact angle and temperature were plotted versus time in Figs. 2 and 3. From the results in Fig. 2, it can be seen that the filler alloy exhibited good wetting ($\theta < 77°$) on 304 stainless steel. At the brazing temperature range of around 970 °C, the filler alloy, Au–18Ni, in molten state, can react with γ-Fe to form a Au-rich peritectic structure. The filler was consumed gradually by γ-Fe in the stainless steel side. This peritectic reaction resulted in a considerably fast wetting process between the filler and the stainless steel. The chromium element in SS 304 also assisted in wetting between the Au–Ni filler and the SS 304 stainless steel due to the eutectic reaction process of

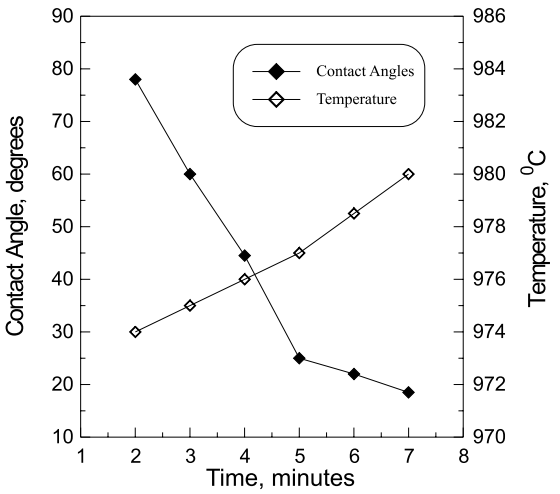

Fig. 2. Wetting experimental results showing time-temperature profile and contact angle on the Au–18Ni filler/SS 304 side.

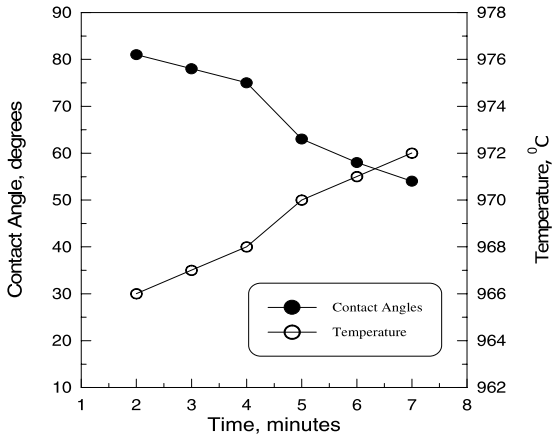

Fig. 3. Wetting experimental results showing time-temperature profile and contact angle on the Au–18Ni filler/V–5Ti–5Cr side.

the binary alloy of Cr–Ni in the brazing temperature range. From the results in Fig. 3, it can be seen that the filler alloy also exhibited good wetting ($\theta < 82°$) on the vanadium alloy side. However, the filler alloy, Au–18Ni displayed slightly difference in wetting capability on the SS 304 stainless steel and on the vanadium alloy, V–5Ti–5Cr. Comparing the results in Figs. 2 and 3, it can be found that the filler alloy showed larger contact angle on vanadium alloy than on the SS 304, which means the wettability of Au–18Ni filler alloy on the V–5Ti–5Cr is not so good as that of the filler on the stainless steel side. It may be explained by the phase diagram of Au–V binary system as given in [58]. The peritetic reaction temperature in the Au–V system is about 240 °C higher than that in the Au–Fe alloy system. This will hinder the wetting process in the Au–Ni/V–5Ti–5Cr side. Thus, the contact angle is larger on this side than that on the stainless steel side at the same time interval.

3.2. Stress–strain relationship

3.2.1. Stress–strain relationship of base materials, V–5Ti–5Cr and stainless steel

The stress–strain curve of the V–5Ti–5Cr, as shown in Fig. 4, displayed an elastic deformation range followed by a non-linear deformation behavior. It can be seen from Fig. 4 that in the small strain range, the relationship between stress and strain is almost linear. The yielding strength reaches about 280 MPa. The calculated value of Young's modulus is about 195 GPa. In the strain range from 1.2% to 3%, the stress–strain relationship is non-linear. Following this range, strain hardening has been observed, corresponding to the strain range of 3–9.5%. The material reached its ultimate strength of 560 MPa. After this range, the tensile strength dropped down and the specimen broke. The strain to failure is about 13%. The stainless steel, SS 304, has higher strength and strain to failure than the V–5Ti–5Cr, as shown in Fig. 4. The SS 304 also shows higher yielding point than the V–5Ti–5Cr does. The ultimate tensile strength of the stainless steel under consideration is about 720 MPa. Its strain to failure reached about 32%. Both materials as base alloys for braze joining demonstrated good plastic deformation capability under the tensile overloading conditions. These properties related to the base alloys will help in explaining the failure behavior of the joints.

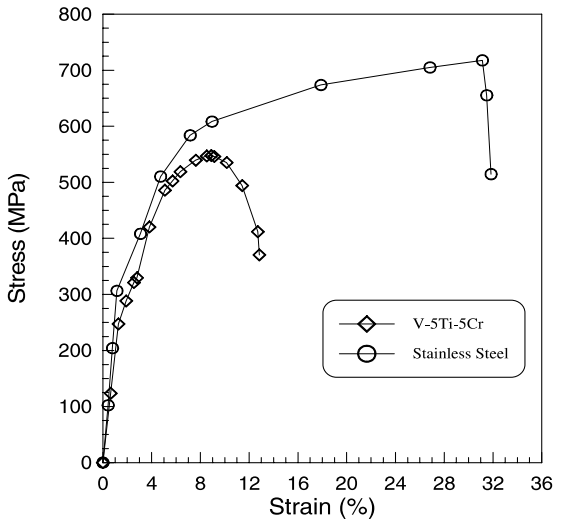

Fig. 4. Stress–stain relationship of the base materials, V–5Ti–5Cr and SS 304 stainless steel.

As compared with the V–5Ti–5Cr in the as-rolled state, the vanadium alloy in as-processed state has lower yield strength and ultimate tensile strength. This indicates that the mechanical properties of V–Ti–Cr alloys are very sensitive to annealing. Specimens directly cut from the as-rolled plate supplied by Wah Chang were also tested using the same MTS 810 under the same loading conditions. The yield strength was about 500 MPa, and the ultimate tensile strength was 620 MPa. The as-processed vanadium alloy was heated up to 970 °C and cooled to room temperature under a considerably small rate (10 °C/min), it can be considered to have been annealed. Similar results have been reported by Smith, Loomis and Diercks for the V-15Cr-5Ti [27]. In their work, it was found that the yield strength and ultimate tensile strength can be reduced to 60–70% of the original values if the annealing temperatures were controlled at 900 °C.

3.2.2. Stress–strain relationship of V–5Ti–5Cr/SS 304 brazed joint

The stress–strain relationship of both unnotched and notched specimens from the V–5Ti–5Cr/Au–Ni/SS 304 joint was generated and shown in Fig. 5. The stress was calculated based on the brazed cross-sectional area before testing. It has been found that the typical unnotched specimen has an ultimate tensile strength of 245 MPa, and maximum strain to failure of about 1.3%. The strength of the brazed joint is less than half of that of the vanadium V–5Ti–5Cr base alloy, and one-third of that of the stainless steel SS 304, as shown in Fig. 4. In the strain range up to 0.3%, the relationship between stress and strain is linear and Young's modulus was about 351 GPa, which is about 75% higher than that of the vanadium and the stainless steel base alloys. In the strain range from 0.3% to 1.3%, the stress–strain relationship displayed non-linear behavior, indicative of limited plastic deformation. The notched specimens showed completely elastic behavior and display much lower tensile strength and strain to failure as compared to the unnotched specimens. The residual strength obtained from typical notched specimen with a/w of 0.46 (notch

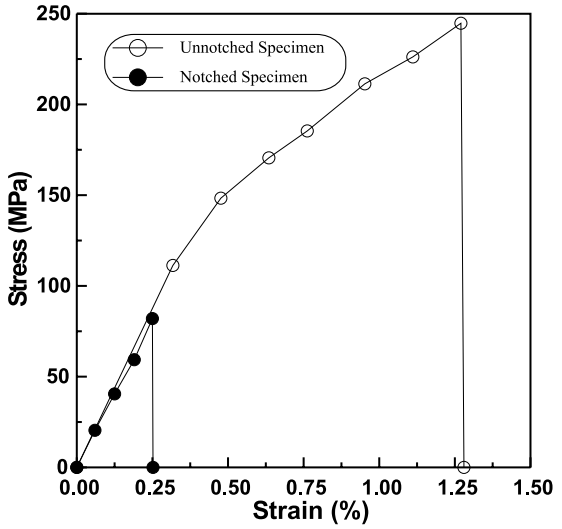

Fig. 5. Stress–stain relationship of both notched and unnotched specimens from the V–5Ti–5Cr/Au–Ni/SS 304 brazed joint.

depth to sample width ratio) is about 82 MPa. This value is about one-third as big as that of the joint without notch. The strain to failure of the notched specimen is only 0.25%. At the point of failure for the specimens from the unnotched brazement, corresponding to the strain of about 1.3% and tensile stress of 245 MPa, the base alloys are still in the elastic deformation range. Thus, the fracture of the brazement occurred in the joint range between the stainless steel and the vanadium alloy.

Brazing experiments using other fillers including MBF80 (Ni7Cr3Fe4·5Si3·2B), Au–Ni–Pd (Au–25Ni–25Pd) and Cu (99.98Cu) were also performed using the same holding time, ramp rate and the cooling rate as shown in Table 1. The brazing temperature for each filler is given in Table 2. For comparison, the tensile property data of several brazed joints and that of the base materials are combined and given in Table 2. These data were obtained under the same test conditions as mentioned before in the experimental section. The results shown in Table 2 indicate that the strength of the joints is much lower than that of the two base materials, V–5Ti–5Cr and stainless steel. A drastic decrease in strain to failure for the four joints is also shown in Table 2. The results indicate that tensile failure occurs on the interfaces between the filler and the base materials. Joints with the other three fillers show much lower tensile strength and strain to failure than the Au–Ni brazement, as can be seen from Table 2. The tensile strength for the joint with MBF80 filler is about 83 MPa. This value is very close to that of the joint with copper as the filler materials, 85 MPa. The joint with Au–Ni–Pd filler alloy demonstrates the lowest tensile strength of 42 MPa. The above analysis indicates that the brazement with Au–18Ni filler can be considered as the most promising joint in view of the tensile properties.

3.3. Fracture toughness

Since the notched brazed joint specimen as illustrated in Fig. 1(b) is subjected to model I tensile loading, according to Irwin [59], the stress intensity factor (K_I) of such configuration can be expressed as follows:

$$K_I = F\sigma_\infty\sqrt{\pi a}, \tag{1}$$

where σ_∞ is the remote stress, F is a geometrical dimensionless factor. For an ideally infinite plate, the value of F is a constant. However, for a plate of finite width W, the stress concentration at the crack tip will increase. With the decrease of W, F increases and consequently K_I will increase. This means that F is a function of (a/w) and the calculation of $F(a/w)$ has been documented in [60].

The stress intensity factor (K_{Ic}) at the critical loading point can be expressed as

$$K_{Ic} = \sigma_c\sqrt{\pi a}F\left(\frac{a}{W}\right), \tag{2}$$

where σ_c is the fracture stress or the residual strength. Obviously, K_{Ic} can be determined based on the residual strength and the given geometrical configuration parameters. In this case, the $F(a/w)$ is in the form as follows [59]:

$$1.12 - 0.23\frac{a}{W} + 10.6\frac{a^2}{W^2} - 21.7\frac{a^3}{W^3} + 30.4\frac{a^4}{W^4}, \tag{3}$$

where σ_c is equal to 82 MPa, and a/w is 0.46 for the V–5Ti–5Cr/SS 304 brazed joint. The calculated value of K_{Ic}

Table 2
Tensile property of base materials and brazed joints

Materials and joints	Base materials		Brazed joints with different filler alloys			
	V5Ti5Cr	SS 304	AuNi	MBF80	AuNiPd	Cu
Processing conditions	as-processed	as-processed	Brazed at 970 °C	Brazed at 1100 °C	Brazed at 1140 °C	Brazed at 1100 °C
Tensile strength (MPa)	550	720	245	83	42	85
Strain to failure (%)	13	32	1.3	0.15	0.16	0.15

equals to 20 MPa $\sqrt{m}$. As for comparison, similar calculation was also performed for the base alloy, V–5Ti–5Cr and the other three joints with MBF80, Au–Ni–Pd and Cu as filler alloys and the results were listed in Table 3. It can be seen from Table 3 that the fracture toughness of the V–5Ti–5Cr is about 110 MPa $\sqrt{m}$, which is about four-and-a-half times higher than that of the Au–Ni brazed joint. The value of K_{Ic} for the stainless steel is expected to be higher than that of the vanadium alloy because the former demonstrated higher plastic deformation strain than the latter as previously shown in Fig. 4. The other three brazements displayed lower fracture toughness than that for the Au–Ni brazed joint. Therefore, the focus of the present study was placed on the Au–Ni joint.

The V–5Ti–5Cr in the as-processed state displayed lower fracture toughness than that of the alloy in the as-rolled state. The as-rolled vanadium has fracture toughness of 124 MPa$\sqrt{m}$ by the same test and calculation procedures as mentioned above. The same trend was also found for the uniform elongation and total elongation. The elongation for the V–5Ti–5Cr was found to be 16% by tensile test, while this value for V–5Ti–5Cr in the as-processed state is only 13%. This means that the vanadium alloy was weakened in a small scale by annealing. Such difference may be explained by the grain boundary segregation and the accumulation of intrinsic interstitial elements such as N, H, and O along the grains boundaries. The exact reason still remains to be found.

3.4. Fracture and failure mechanisms

The fracture surface of the V–5Ti–5Cr after static testing was observed using scanning electron microscopy and the morphology is shown in Fig. 6. The fracture surface is featured by vertically elongated grains, intergranular voids, cleavage facets, indicating a mixed ductile–brittle fracture mechanism under the overloading conditions. The fracture morphology of the two counterpart surfaces of the V–5Ti–5Cr/Au–Ni/304 stainless steel was also examined. The residual of the filler material, Au–Ni, can be seen in the form of white areas or spots. Such feature is illustrated in Figs. 7(a) and (b) for the vanadium side and stainless steel side, respectively. It can be seen from Fig. 7(a) that the surface is covered

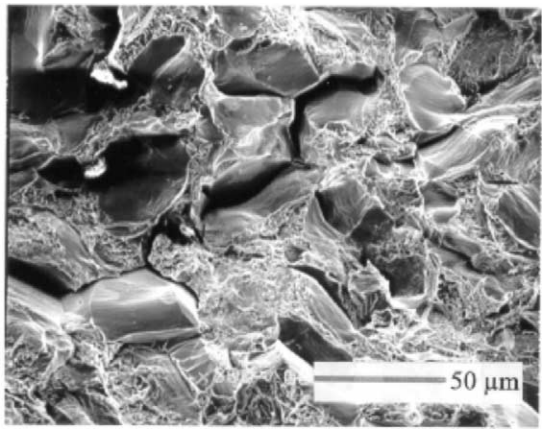

Fig. 6. SEM micrograph showing the fracture surface of static failed V–5Ti–5Cr with the major features of elongated grains, intergranular voids, and cleavage facets.

with the filler material and the microstructure demonstrates fairly porous texture underneath the white spots from the filler materials. Such porosity indicates the improperly wetted locations which can be taken as brazing defects. The white spots represent well-brazed area with good wettability. In these areas, considerably large pieces of material due to the solidification of residual liquid filler alloy of Au–Ni and/or iron based solid solution can be readily found on the surface, as shown by the white area in the SEM micrograph of Figs. 7(a) and (b) which shows the fracture surface on the stainless steel side. Unlike the feature shown in Fig. 7(a), the base material, 304 stainless steel, is almost veiled by the filler alloy of Au–Ni with much less porosity. The filler appears to be completely absorbed by the stainless steel substrate with the formation of very fine structure. Thus, the stainless steel side shows more uniform texture than the vanadium side does, indicating better wettability between the filler and the SS 304. This is in accordance with the results shown in Figs. 2 and 3 on the wetting behavior of the filler and the substrate materials. As mentioned in the previous section, the strength of the brazement, 245 MPa, is far below the tensile strength of both V–5Ti–5Cr and SS 304, the initiation site of the crack should be inside the joining region. The SS 304/filler interface showed better wettability than the vanadium/filler interface did. Therefore, the failure tends to

Table 3
Fracture toughness of V–5Ti–5Cr alloy and the brazed joints

Base materials and brazed joints	V–5Ti–5Cr as-processed	Brazed joints with different filler alloys			
		AuNi	MBF80	AuNiPd	Cu
Fracture toughness K_{Ic} (MPa $\sqrt{m}$)	110	20	1.7	2.1	11

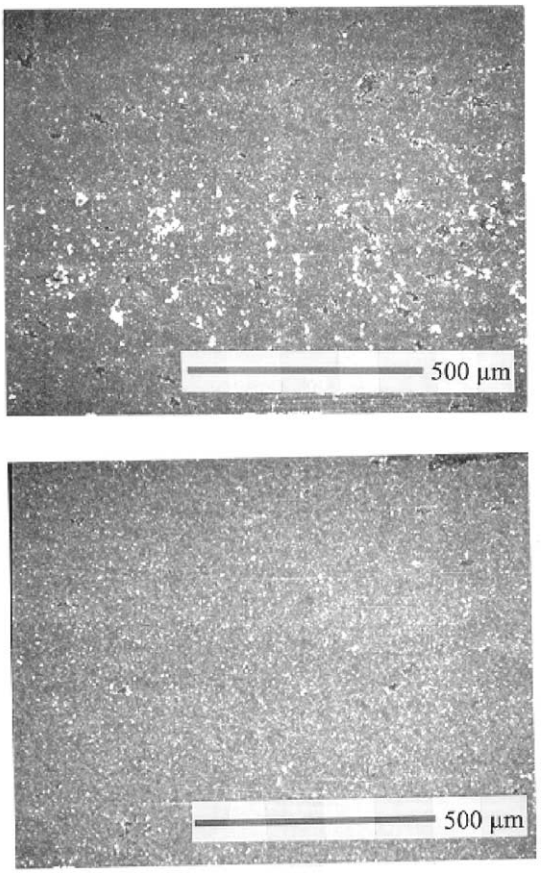

Fig. 7. Fracture surfaces of brazed V–5Ti–5Cr/304 stainless steel joint with Au–Ni filler: (a) V–5Ti–5Cr side; (b) stainless steel side.

occur along the interfacial area between V–5Ti–5Cr and the Au–Ni filler alloy.

4. Conclusions

The fracture toughness and mechanical properties of vanadium to stainless steel joints brazed with Au–Ni filler were studied. The stress–strain relationship of the brazed joint displayed elastic deformation dominated behavior. Its ultimate tensile strength reached about 245 MPa. The strain to failure is about 1.3%. Young's modulus is about 351 GPa. The fracture toughness (K_{Ic}) of this joint is 20 MPa $\sqrt{m}$, which is about one-fifth of that of the vanadium base alloy, 110 MPa $\sqrt{m}$.

Microstructural features of the fractured joint with the Au–Ni filler alloy were correlated with the mechanical properties and fracture toughness. The fracture surface of the joint from the vanadium side exhibited fairly porous texture with spots of solidified filler alloy. The stainless steel side, on the other hand, displayed a fine texture with very limited porosity. The filler appears to be largely dissolved. On this basis, the failure of the joint can be considered to occur in the interface of the vanadium/filler side.

Acknowledgements

This work was supported by US Department of Energy (grant No. DE-FG02-96ER54384).

References

[1] M. Rodij, R. Conrad, H. Derz, G. Vieider, J. Nucl. Mater. 283–287 (2000) 1161.
[2] C.H. Carden, B.C. Odegard Jr., J. Nucl. Mater. 283–287 (2000) 1253.
[3] B. Odegard, B. Kalin, J. Nucl. Mater. 233–237 (1996) 44.
[4] B. Odegard, C.H. Carden, R. Walson, K. Slattery, J. Nucl. Mater. 258–263 (1998) 329.
[5] G. Alexander, M. Igor, Y. Nikolai, G. Anatoly, Fus. Technol. 38 (2000) 277.
[6] B. Kalin, V. Fedotov, O. Seuryukov, A. Plyuschev, I. Mazal, A. Gerash, R. Giniatulin, J. Nucl. Mater. 271&272 (1999) 410.
[7] Y. Han, C. Park, K. Jang, C. Bae, C. Choi, J. Lee, J. Nucl. Mater. 270 (1999) 334.
[8] A. Pizzuto, B. Riccardi, E. Salpietro, G. Malavasi, Fus. Eng. Des. 27 (1995) 382.
[9] M. Akiba, S. Suzuki, Fus. Eng. Technol. 39&40 (1998) 219.
[10] M. Rodig, R. Duwe, C. Ibbott, D. Jacobson, G.L. Marois, A. Lind, J. Linke, P. Lorenzetto, A. Peacock, L. Plochl, A. Schuster, Y. Severi, G. Vieider, E. Visca, B. Wiechers, Fus. Eng. Technol. 39&40 (1998) 551.
[11] C. Park, Y. Han, Y. Kim, K. Jang, J. Lee, C. Choi, K. Sim, J. Nucl. Mater. 254 (1998) 34.
[12] J.H. Yo, Fus. Eng. Technol. 38 (1998) 295.
[13] J.H. Yo, G. Breitbach, Fus. Eng. Technol. 38 (1998) 307.
[14] W. Hohenauer, H. Bolt, T. Koppitz, J. Linke, R. Lison, J.H. Yo, H. Nickel, Fus. Eng. Technol. 38 (1998) 319.
[15] J.H. Yo, H. Bott, R. Duwei, J. Linke, H. Nickel, J. Nucl. Mater. 250 (1997) 184.
[16] A. Anisimov, V. Frolov, V. Komarov, I. Mazul, S. Moszherin, G. Pepekin, A. Pirogov, Fus. Eng. Des. 37 (1997) 253.
[17] C.H. Carden, B.C. Odegard, Fus. Eng. Des. 37 (1997) 287.
[18] T. Tanabe, V. Philipps, K. Nakamura, M. Fujine, Y. Ueda, M. Wada, B. Schweer, A. Pospieszezyk, B. Unterberg, J. Nucl. Mater. 241–243 (1997) 1164.
[19] H.K. Lee, J.Y. Lee, J. Mater. Sci. 31 (1996) 4133.
[20] S.D. Pereves, M. Paulasto, G. Ceccone, V. Stamos, Acta Mater. 46 (1998) 2407.
[21] L. Giancarli, J.P. Bonal, A. Caso, G.L. Marois, N.B. Morley, J.F. Salavy, Fus. Eng. Technol. 39&40 (1998) 165.
[22] H. Ise, S. Satoh, S. Yanazaki, M. Akiba, K. Nakamura, S. Suzuki, M. Araki, Fus. Eng. Technol. 39&40 (1998) 5.
[23] R.J. Kurtz, K. Abe, V.M. Chernov, V.A. Kazakov, G.E. Lukas, H. Matsui, T. Muroga, G.R. Odette, D.L. Smith, S.J. Zinkle, J. Nucl. Mater. 283–287 (2000) 70.

[24] S.N. Votinov, M.I. Solonin, Y.I. Kazennov, V.P. Kondratjev, A.D. Nikulin, V.N. Tebus, E.O. Adamov, S.E. Bougaenko, Y.S. Strebkov, A.V. Sidorenkov, V.B. Ivanov, V.A. Kazakov, V.A. Evtikhin, I.E. Lyublinski, V.M. Trojanov, A.E. Rusanov, V.M. Chernov, G.A. Birgevoj, J. Nucl. Mater. 233–237 (1996) 370.
[25] D.L. Smith, B.A. Loomis, D.R. Diercks, J. Nucl. Mater. 135 (1985) 125.
[26] W. Rostoker, in: The Metallurgy of Vanadium, Wiley, New York, 1958, p. 139.
[27] Teledyne, Wah Chang, Albany, Materials Safety Data Sheet: Vanadium–Titanium–Chromium Alloys, No. 986, Albany, OR, 1992, p. 1.
[28] M.L. Grossbeck, J.F. King, in: Fusion Materials, Semi-Annual Progress Report for Period Ending June 1999, DoE/ER-0313/26, 1999, p. 44.
[29] M.L. Grossbeck, J.F. King, D.T. Hoelzer, in: Proceedings of the 4th IEA Workshop on Vanadium Alloys for Fusion Applications, Argonne National Lab, Chicago, IL, 1999, p. 1356.
[30] M.L. Grossbeck, J.F. King, in: Proceedings of the 4th IEA Workshop on Vanadium Alloys for Fusion Applications, Argonne National Lab, Chicago, IL, 1999.
[31] N.B. Potluri, M.L. Grossbeck, H. Aglan, B.A. Chin, Investigation on embrittlement of V–4Ti–4Cr alloy during fusion welding, in: Presentation on Conference: Trends in Welding '98.
[32] K. Natesan, D.L. Smith, P.G. Sanders, K.H. Leong, Semi-annual progress report for period ending December 1997, DoE/ER-0313/23, 1998, p. 136.
[33] K. Natesan, D.L. Smith, Z. Xu, K.H. Leong, Semi-annual progress report for period ending June 1998, DoE/ER-0313/24, 1998, p. 87.
[34] K. Natesan, C.B. Read, Z. Xu, D.L. Smith, Semi-annual progress report for period ending 1998, DoE/ER-0313/25, 1999, p. 64.
[35] Z. Xu, C.B. Read, K. Natesan, D.L. Smith, Semi-annual progress report for period ending June 1999, DoE/ER-0313/26, 1999, p. 49.
[36] W.R. Johnson, P.W. Trester, in: Proceedings of the 4th IEA Workshop on Vanadium Alloys for Fusion Applications, Argonne National Lab., Chicago, IL, 1999.
[37] Z. Xu, C.B. Read, D.L. Smith, Semi-annual progress report for period ending June 1999, DoE/ER-0313/26, 1999, p. 54.
[38] R.V. Steward, MS Thesis (Advisor, Dr. B.A. Chin), Auburn University, Auburn, AL, 1998.
[39] J.Y. Liu, S. Chen, B.A. Chin, J. Nucl. Mater. 212 (1994) 1590.
[40] R.V. Steward, M.L. Grossbeck, B.A. Chin, H. Aglan, Y. Gan, in: Proceedings of the 4th IEA Workshop on Vanadium Alloys for Fusion Applications, Argonne National Lab., Chicago, IL, 1999.
[41] R.V. Steward, M.L. Grossbeck, B.A. Chin, H. Aglan, Y. Gan, J. Nucl. Mater. 283–287 (2000) 1224.
[42] M.M. Schwartz, Brazing, ASM International, Metals Park, OH, 1990, p. 164.
[43] G. Sheward, High Temperature Brazing in Controlled Atmospheres, Pergamon, Oxford, 1985, p. 3.
[44] E.F. Nippes (coordinator), ASM Handbook Committee, and ASM Joining Division Council, Welding, Brazing, and Soldering, American Society for Metals, Metals Park, OH, 1983, p. 593.
[45] W.D. Zhuang, T.W. Eagar, Weld. J. 76 (1997) 526.
[46] R.L. Peaslee, Weld. J. 76 (1997) 106.
[47] T. Noda, T. Shimizu, M. Okabe, T. Iikubo, Mater. Sci. Eng. A 240 (1997) 613.
[48] R.L. Peaslee, Weld. J. 76 (1997) 272.
[49] W. Tillmann, E. Lugscheider, K. Schlimbach, C. Manter, J.E. Indacochea, Weld. J. 76 (1997) 300.
[50] D. Huh, D.H. Kim, J. Mater. Res. 12 (1997) 1048.
[51] T.H. Schubert, W. Loser, A. Teresiak, N. Mattern, H.D. Bauer, J. Mater. Sci. 32 (1997) 2181.
[52] F. Stantonin, M. Suery, P. Meneses, G. Lemarois, F. Moret, J. Nucl. Mater. 237 (1996) 935.
[53] B.A. Kalin, V.T. Fedotov, O.N. Sevryukov, A.E. Grigoryev, A.N. Plyuschev, V.M. Ivanov, Y.S. Strebkov, J. Nucl. Mater. 237 (1996) 945.
[54] P.K. Vallittu, J. Oral Rehabilitation 24 (1997) 444.
[55] Z.Y. He, L.P. Ding, Mater. Chem. Phys. 49 (1997) 1.
[56] W.P. Weng, T.H. Chuang, Metall. Mater. Trans. A 28 (1998) 2673.
[57] T. Yamazaki, A. Suzumura, J. Mater. Sci. 33 (1998) 1379.
[58] E.F. Nippes (coordinator), ASM Handbook Committee, and ASM Joining Division Council, Metals Handbook, Metallography, Structures and Phase Diagram, American Society for Metals, Metals Park, OH, 1973, p. 269.
[59] G.R. Irwin, J. Appl. Mech. 24 (1957) 361.
[60] K. Hellan, Introduction to Fracture Mechanics, McGraw-Hill, New York, 1984, p. 244.